J Mater Sci (2008) 43:1002–1007
DOI 10.1007/s10853-007-2247-9

Hot pressing of hafnium diboride aided by different sinter additives

Frederic Monteverde

Received: 13 June 2007 / Accepted: 22 October 2007 / Published online: 15 November 2007

Abstract Experiments were conducted by hot-pressing to densify HfB_2 commercial powders using $HfSi_2$ (5 vol%) or B_4C (7 vol%) as sinter additives. The former was very effective as sintering enhancer: 15 min at 1,600 °C was a sufficient condition to achieve near full density. The occurrence of a liquid phase sintering, which substantially enhanced densification during hot-pressing, was found out. The HfB_2–B_4C powder mixture, hot-pressed at 1,900 °C for 40 min, achieved a relative density of 94%. Aside the key role of sintering enhancer, B_4C also allowed the development of a uniform microstructure, preventing an excessive growth of the diboride matrix (2 μm mean size). On the contrary, thanks to the liquid phase that sustained substantial transfer of mass during heating, the $HfSi_2$-doped composition had an uneven and more obvious grain growth (4 μm mean size), with faceted diboride grains up to 10 μm.

Introduction

The development of a new generation of space vehicles is currently reviving an impressive interest into a special class of highly refractory materials such as the ultra-high temperature ceramics (UHTCs) for use in advanced aerospace [1], as well as in critical ground-based applications [2]. Diborides of group IVb transition metals are being attracting considerable attention, with HfB_2 and ZrB_2 as the most studied candidates [2].

In the majority of studies reported, the densification of HfB_2 compacts was undertaken through hot-pressing: due to the covalent character of chemical bondings as well as low grain boundary/volume diffusion rates, densification of undoped diboride powders has been satisfactory only under sustained conditions of temperature and pressure. An early attempt to densify HfB_2 by hot-pressing was carried out by Kalish and Clougherty [3]: they obtained fully dense samples only when the temperature exceeded 1,840 °C under a pressure of 800 MPa. Wuchina and co-workers coupled reactive sintering and hot-pressing using elemental powders of Hf and B [4]: although this approach had beneficial effects on densification with residual porosity between 5 and 10%, it nevertheless required sustained processing conditions of temperature (i.e., 2,160 °C) and dwell time (i.e., 180 min). More recently, Loehman R. et al. processed pure HfB_2 powders by hot-pressing at 2,000 °C for 60 min (34 MPa of applied pressure), reaching a fractional relative density not exceeding 70% [5]. Others groups are currently evaluating the feasibility of "in-situ" low-temperature reactions using organic–inorganic precursors which allow for the formation of structures to be processed under pressureless or mild-pressure conditions at more suitable processing temperatures [6]. Attempts to densify undoped HfB_2 by spark plasma sintering were unsuccessful as well [7, 8].

The oxygen contamination has been recognized as the primary serious detriment for the densification of HfB_2 powders. Oxide impurities located upon the diboride particles surfaces promote neck formation and particle coarsening at high temperature by vapor/surface transport mechanisms that are scarcely effective for densification. Sinter additives expected to enhance densification have been used. Refractory metals [9] and metal silicides [10], used with the function of liquid phase formers (LPFs),

---

F. Monteverde (✉)
ISTEC-CNR, Institute of Science and Technology
for Ceramics - National Research Council, Via Granarolo 64,
48018 Faenza, Italy
e-mail: fmonte@istec.cnr.it

clearly aided densification and reduced processing temperatures. Differently from LPFs, reactive agents may act as densification aid by removing oxygen through solid state reactions at the reacting interfaces. Only attempts to densify ZrB_2 with reactive additives like carbon [11] or B_4C [12] were reported.

In this perspective, the present work addressed the suitability of B_4C (i.e., reactive agent) and $HfSi_2$ (i.e., LPF) as effective sinter enhancers for commercial HfB_2 powders through hot-pressing. As for the selection of similar sintering aids, bases were given in the Results/Discussion section.

Experimental

In order to verify the suitability of two different sinter enhancers for HfB_2 commercial powders, the following powders mixtures (vol%)

$HfB_2 + 5HfSi_2$ (composition HFHS)

$HfB_2 + 7B_4C$ (composition HFBC)

were ball-mixed in absolute ethyl alcohol using SiC balls, dried in a rotating evaporator, and sieved through a mesh screen with 250 μm openings. Powders of HfB_2 (11.18 g/cm^3 density, 99.5% pure, 325-mesh type, FSSS 1.7 μm, Cerac Inc.—USA) and B_4C (2.52 g/cm^3 density, 97% pure, grade HS, 15–20 m^2/g specific surface area, H.C. Starck—Germany) were used. For the $HfSi_2$ synthesis (7.97 g/cm^3 density), commercial solid precursors of Hf (99.8% pure, FSSS 2.1 μm, Neomat Co.—Latvia,) and Si (grade AX05 99.9% pure, FSSS 3.5 μm, H.C. Starck—Germany) were selected. While purity values are those declared by the producers, the total content of oxygen and carbon in the processed powder mixtures was measured by combustion technique. According to the expected Si to Hf atomic ratio of $HfSi_2$, the correspondent mixture of Hf + 24wt%Si was ball-mixed for 2 days in *n*-hexane (SiC balls) to favor intimate mixing of reactants. Individual heat treatments were conducted in flowing Argon, adjusting the end-temperature in the range 900–1,350 °C (50 °C increasing step), 10 °C/min of heating rate and 45 min of dwell time, using a furnace (Astro Industries Inc.—USA) heated with graphite elements. Compacted pellets of the as-mixed Hf–Si powder (about 2.5 g in weight, 15 mm in diameter) were isostatically cold-pressed at 350 MPa, and then placed inside a graphite crucible. The heat treated pellets were then finely crushed in an agate mortar, and analyzed through X-ray diffraction (XRD, Ni-filtered CuKα radiation, mod. D500, Siemens—Germany). A detailed description of the $HfSi_2$ powder batched in the HFHS formulation is reported in the Results/Discussion section.

The powder mixtures HFHS and HFBC were uniaxially hot-pressed in an actively pumped vacuum (1.5 mbar) using an inductively heated graphite die, 30 MPa of applied pressure. For each composition, a quantity of about 90 g was put inside the graphite die (44 mm inner diameter) lined with a BN-sprayed graphitized sheet. The average heating rate was about 20 °C/min. Peak temperatures and dwell times are listed in Table 1. Only for the hot-pressing associated to composition HFBC, an intermediate hold of 30 min at 1,450 °C was done. The temperature was measured by means of an optical pyrometer focused on the graphite die. Bulk density was determined using the Archimedes' method, water as an immersing medium. The phase composition was analyzed with an X-ray diffractometer together with a scanning electron microscope (SEM, mod. S360, Leica Cambridge—UK) combined with an energy dispersive X-ray microanalyser (EDS, mod. INCA Energy 300, Oxford Instruments—UK). Polished sections of the as-sintered materials were prepared with successively finer diamond-based abrasives down to 0.25 μm. According to the standard procedure ENV 623-5, the amount of the residual porosity, as well as of some secondary phases, was determined using SEM images.

Results and discussion

The synthesis of $HfSi_2$

Based on the XRD outputs, the formation of $HfSi_2$ (ICDD 38-1373) proceeded to a certain extent at 1,000 °C, until

Table 1 Processing conditions and typical parameters during hot-pressing: total content of oxygen (O ± 0.02wt%) and carbon (C ± 0.02wt%), onset temperature of some measurable shrinkage (T_{ON}, °C), peak temperature (T_P, °C), dwell time (d_W, min), shrinkage rate (V_P, min/min) at T_P, shrinkage rate (V_F, mm/min) at the dwell end, bulk density (ρ_B ± 0.02, g/cm^3), residual porosity (P ± 0.5%) and mean grain size (mgs, μm)

Label	Additive	^{a}O	^{a}C	T_{ON}	T_P	d_W	V_P	V_F	ρ_B	^{b}P	mgs
HFHS	$HfSi_2$	0.71	0.07	1,340	1,600	15	0.08	<0.005	10.8	^{c}	4 ± 1
HFBC	B_4C	0.65	–	1,700	1,900	40	0.36	0.01	10	6	2 ± 0.2

^{a} By combustion technique (LECO); ^{b} By image analysis; ^{c} Not measurable; –not determined the consumption of Silicon, according to the XRD resolution, seemed complete at 1,150 °C (45 min dwell time). The heat treatment at 1,150 °C ensured the lowest process temperature in conjunction with an easy-to-crush final product. Only the $HfSi_2$ powder synthesized at 1,150 °C was further comminuted for 20 min using a planetary agate mill using SiC milling media, and sieved (25 μm openings) to remove coarse hard agglomerates. This powder was used for further hot-pressing.

Hot-pressed materials: densification and microstructure development

While B_4C [12] and some metal silicides [13, 14] displayed a valuable potential as sinter additive for developing diboride-based materials designed to high temperature applications, only one attempt to process a powder mixture of HfB_2 + 7 vol% $HfSi_2$ via hot-pressing was reported [10]. Aside the effective role of the silicide as sintering enhancer for metal diborides, the present HfB_2–$HfSi_2$ system showed the potential to transform the oxide impurities of the original processed HfB_2 powders into HfB_2 (see further discussion). In addition, the oxidation resistance of metal diboride matrices (not object of this work) is expected to take advantage from the presence of Si-containing phases because at high temperatures they generate a silica-based glassy barrier against the oxygen diffusion [13, 15]. On the contrary, although separate authors showed the ability of B_4C to convert the metal oxide impurities of some metal diboride powders into the same metal diboride constituting the powder [12, 16], any published data relate to the addition of B_4C to HfB_2.

In the present work, densification behaviors during hot-pressing are shown in Fig. 1: compared to B_4C, the impact of $HfSi_2$ as effective additive at much lower temperature on the densification of HfB_2 is apparent. The onsets of some measurable shrinkage of HFHS and HFBC compositions occurred at 1,340 and 1,700 °C, respectively. The sudden rise just above 1,340 °C in the shrinkage pattern of the HFHS composition was associated to the occurrence of a liquid phase sintering (see further discussion). On the contrary, the addition of B_4C started having an appreciable effect on the sample shrinkage only for temperatures in excess of 1,750 °C (Fig. 1a) and for a longer dwell time (Fig. 1b). For the HFHS composition, the isothermal stage of 15 min at 1,600 °C was sufficient to achieve nearly full density. However, the HFBC composition required a prolonged exposure to much higher temperatures to achieve an acceptable level of densification (Table 1).

SEM investigations revealed a differing development of the resulting microstructures (Fig. 2). In the HFHS composition residual porosity was not seen; however, although a (moderate) peak temperature of 1,600 °C was applied, an appreciable grain growth took place, and diboride grains up to 10 μm were found. In addition, contrary to the HFBC material which exhibits a transgranular fracture, the typical fracture of the HFHS material is intergranular (Fig. 2). The XRD analysis, the hexagonal HfB_2 phase apart in both the hot-pressed samples, identified monoclinic HfO_2 (3.7 ± 0.3 vol%) and cubic HfC in the only HFHS sample. By using SEM-EDS, other secondary phases were found in the HFHS sample (Fig. 3): discrete Si-based pockets (4.5 ± 0.4 vol%) and residual $HfSi_2$ (<1 vol%). The quantities of these secondary phases were determined through SEM image analyses. In the case of HfC, its phase contrast very similar to that of the diboride matrix did not allow to count it appropriately. Such a carbide, according to the reaction $HfO_2 + 3C = HfC + 2CO(g)$ having a negative Gibbs free energy above 1,000 °C (1.5 mbar of total pressure), formed during hot-pressing, thanks to the carbon impurity introduced during powder processing (Table 1). The wear involving inner surfaces of the polyethylene jar and hard media/powders particles is expected to introduce C-based adsorbates in the processed batches [17].

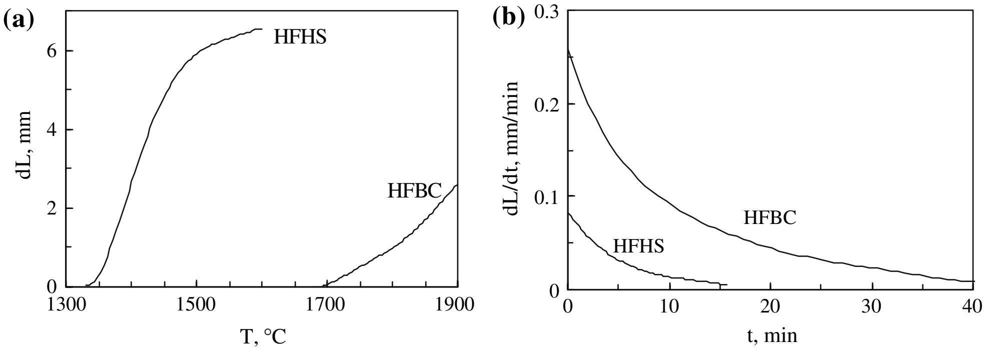

Fig. 1 Hot-pressing of HFHS and HFBC compositions: shrinkage dL vs. temperature T (**a**, heating stage), and shrinkage rate dL/dt vs. time t (**b**, isothermal hold)

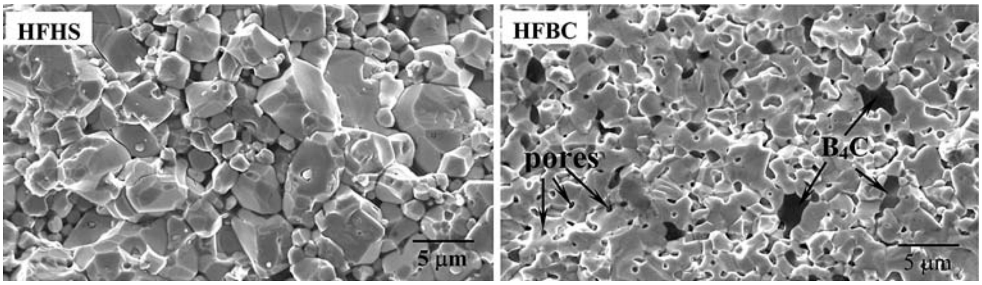

Fig. 2 Fracture surfaces of materials HFHS and HFBC (SE-SEM micrographs)

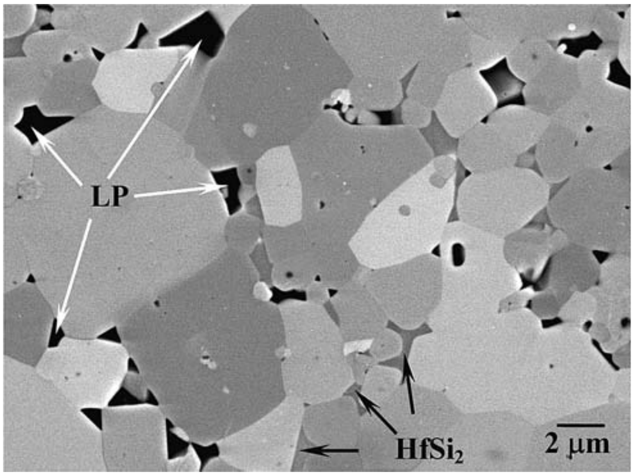

Fig. 3 Material HFHS (BSE-SEM micrograph, polished section): Si-based pockets (LP) and residual $HfSi_2$ are indicated

The Si-based compound remaining upon cooling very likely discloses the occurrence of a liquid-phase sintering. The formation of a liquid phase at temperatures above 1,340 °C readily provided diffusion paths for an enhanced mass transport. It can first be stressed that the Hf–Si phase diagram has an eutectic point at 1,350 °C when the mole fraction of Silicon exceeds 0.9: this is consistent with an onset temperature of about 1,340 °C lower than the melting point of Si (1,414 °C). Hafnium found in the Si-based pockets (Fig. 4) strengthens the inference of a liquid phase sintering as consequence of the partial dissolution of HfB_2 into the Si-based liquid phase. EDS spectra in Fig. 4 were acquired at 4 keV of electron beam energy: this condition ensures an enhanced sensitivity to light elements and a maximum beam broadening of 0.2 µm inside the selected areas [18]. Such a value results lower than the typical size of the Si-based pockets (i.e., a few microns). An eventual residue of Boron falls below the detection limit of the technique used.

In addition, the finding of a residual intergranular thin film between adjacent diboride grains (Fig. 5) further consolidates the reasoning that a liquid phase sintering has contributed to densification not only by re-arranging grains through a capillary action, but also via a substantial mass transfer. Actually, the liquid phase sintering promoted the growth of relatively large grains at expenses of the original smaller ones: the resultant microstructure in fact exhibits a broad grain size distribution. Due to the AlB_2-type crystal structure of HfB_2, the grain coarsening (boosted by the liquid-phase) facilitated faceted grains to grow rapidly, leaving sometimes trapped pores within the larger grains (Fig. 3).

A melting point of $HfSi_2$ (close to 1,700 °C) lower than the peak temperature operated during hot-pressing, the major portion of shrinkage in the temperature range 1,300–1,500 °C (see Fig. 1), shape and little amount of the

Fig. 4 EDS spectra of Si-based pockets (left), or of residual $HfSi_2$ (right)

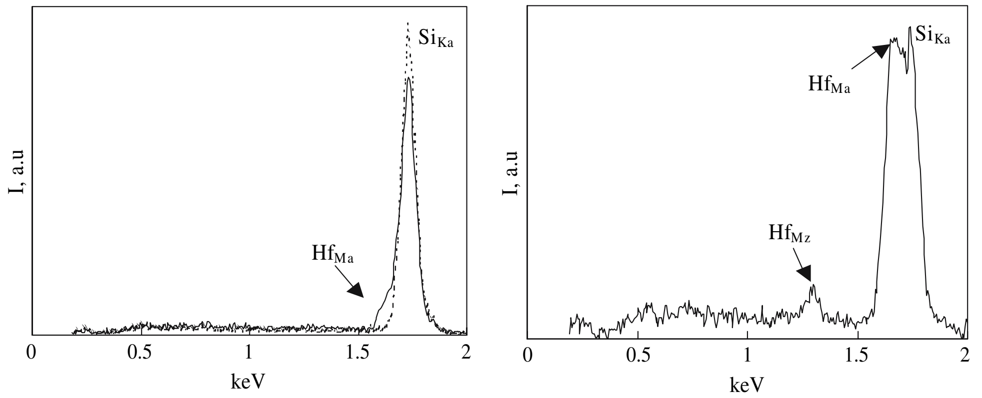

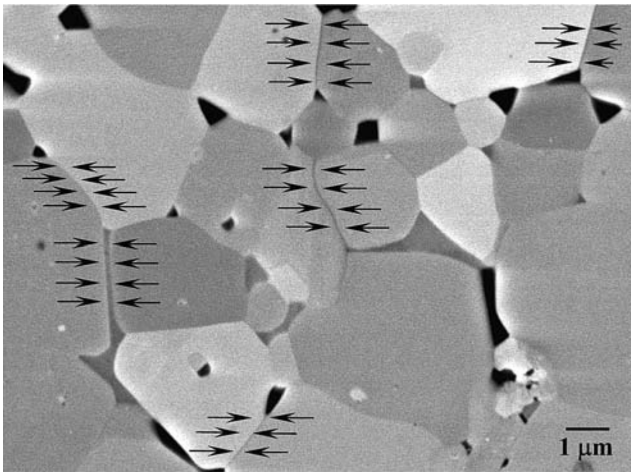

Fig. 5 HFHS material (BSE-SEM micrograph, polished area): an intergranular thin phase is indicated

residual $HfSi_2$ particles: these remarks tend to exclude a major contribution to liquid phase sintering from the melting of $HfSi_2$. Instead, the origin of the liquid phase was looked into the reaction involving $HfSi_2$ and the oxygen-bearing species typically present on the diboride particle surfaces. In fact, the existing Hf–Si–B phase diagram [19] shows compatibility between HfB_2 and $HfSi_2$ at 1,300 °C. Therefore, the reaction

$$5HfSi_2 + 2B_2O_3 = 2HfB_2 + 10Si + 3HfO_2$$

(negative Gibbs free energy in the temperature processing range) was hypothesized to occur. According to other authors [2, 17], surface oxides impurities were postulated to exist as a mixture of B_2O_3 and HfO_2. However, supported by Bronson and co-workers [10] which found $HfSi_2/HfO_2$ interface not moving (i.e., not reacting) at 1,600 °C, a contribution from the HfO_2 component in the origin/formation of the liquid phase has not found valuable confirmations.

The incorporation of B_4C as additive in the HFBC composition influenced densification and grain growth of HfB_2. Pure HfB_2 powders, hot-pressed at 2,000 °C and 35 MPa for 60 min [5] or spark plasma sintered at 1,900 °C at 95 MPa for 10 min [7] reached relative densities not exceeding 70 and 87%, respectively. In the case herein discussed, compared to HFHS material, a finer and more regular final texture was obtained. Residual porosity (6 ± 0.5%) and isolated B_4C particles (3 ± 0.5%) were also seen (Fig. 6). Similarly to other metal diborides like ZrB_2 [12] or TiB_2 [20], the presence of B_4C facilitated the removal of surface oxides from the HfB_2 powder particles at temperatures low enough to prevent significant coarsening of the metal diboride. As a consequence, boundary/volume mass transport mechanisms involved the re-activated diboride surface particles (i.e., depleted of the densification inhibitors like the surface oxides), and

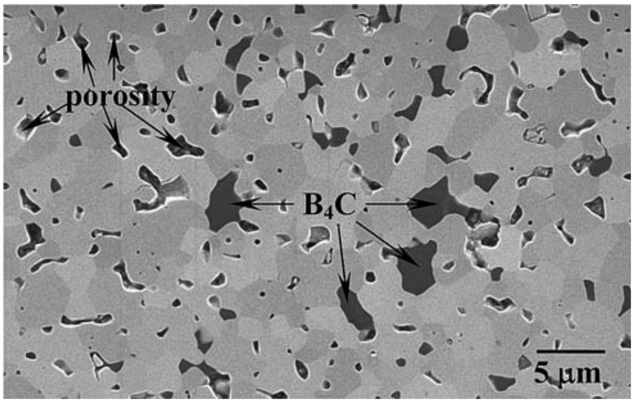

Fig. 6 HFBC material (BSE-SEM micrograph, polished area): larger B_4C particles and some porosity are indicated

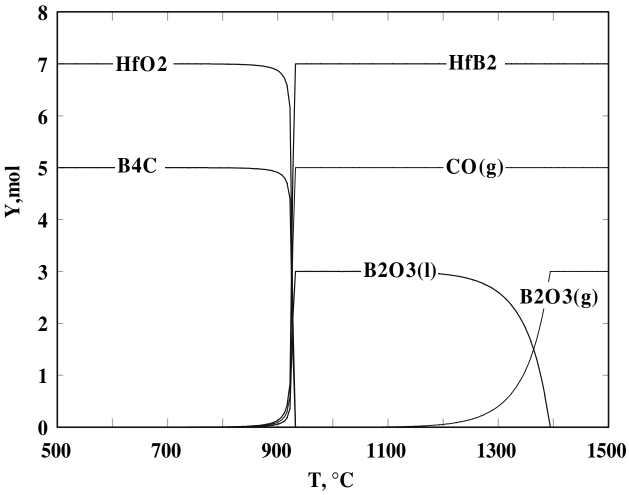

Fig. 7 Equilibrium amount (Y) calculated by HSC [21]: $7HfO_2$ and $5B_4C$ as starting amounts, 1.5 mbar of total pressure

dominated over surface-to-surface mass transfer mechanisms. The reaction

$$7HfO_2 + 5B_4C = 7HfB_2 + 5B_2O_3(l,g) + CO(g)$$

(thermodynamically favored for temperature above 900 °C and 1.5 mbar of total pressure (Fig. 7)) was thought to drive the conversion of HfO_2 into HfB_2. Such a transformation is further accompanied by the loss of volatile boron oxide that easily evaporates due to its equilibrium vapor pressure (i.e., 36 mbar at 1,450 °C) well above the pressure of the processing environment of 1.5 mbar.

The reactivity between B_2O_3 and B_4C, the former being the other phase composing the surface oxide, was considered from the thermodynamic point of view. Depending on the total equilibrium pressure and temperature, B_2O_3 and B_4C may interact giving rise to Boron and volatile products (Fig. 8). Reaction should take place for total pressure >2.5 mbar at 1,450 °C: for this, a reaction involving B_2O_3 and B_4C during the hold at 1,450 °C was deemed unlikely.

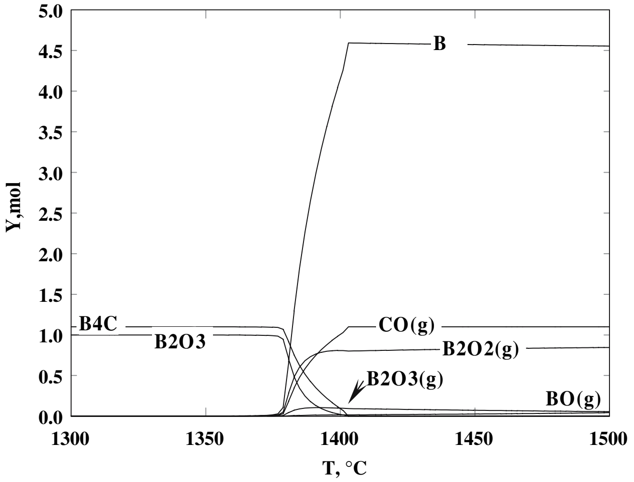

Fig. 8 Equilibrium amount (Y) calculated by HSC [21]: $1B_2O_3$ and $1.1B_4C$ as starting amounts, 1.5 mbar of total pressure

In addition, the existence of residual solid B_4C particles in the sintered HFBC sample verified that the thermodynamic conditions for a reduction of B_2O_3 through B_4C were not fully established. The hold of 30 min at 1,450 °C during hot-pressing actually served to minimize as well the oxygen activity of the surface oxides through the volatilization of boron oxides. In connection with that, the actively pumped hot press chamber, monitored with a Pirani vacuum gauge, showed a measurable decrease at 1,350 °C from 2 to 3 mbar and then recovered a value of 1.5 mbar at the end of the intermediate stage at 1,450 °C.

The presence of B_4C, according to Zhang et al. that studied the ZrB_2–B_4C system [12], had the aforesaid benefit to convert oxide impurities into HfB_2. In addition, the un-consumed B_4C played also the role of grain growth inhibitor at high temperature, preventing excessive coarsening which however occurred in the HFHS composition at significantly lower temperatures.

Conclusions

Sinterability of commercial metal diboride powders is adversely affected by the surface oxides on the original processed particles. Growing evidence of enhanced sinterability of HfB_2 through hot-pressing was provided, thanks to the addition of sinter enhancers like B_4C (7 vol%) and $HfSi_2$ (5 vol%). The former helped densification of the HfB_2 powder by promoting the removal of its surface oxide contamination: this provided an enhanced high temperature reactivity to the HfB_2 matrix that reached a bulk density of 10 g/cm^3, 6% of residual porosity. $HfSi_2$, differently from B_4C, controlled the removal of the surface oxide impurities through a Si-based liquid phase that allowed full densification at 1,600 °C, a temperature much lower than that used for B_4C (i.e., 1,900 °C). Differing microstructures resulted after hot-pressing. B_4C in fact, aside the role of sintering enhancer, prevented also an excessive growth of the diboride matrix (2 μm mean size). On the contrary, thanks to the liquid phase sintering that sustained substantial transfer of mass, the $HfSi_2$-doped composition had a more obvious grain growth (4 μm mean size), with faceted diboride grains up to 10 μm.

References

1. Rapp R (2006) Mater Today 9(5):6
2. Fahrenholtz WG, Hilmas GE, Talmy IG, Zaykoski JA (2007) J Amer Ceram Soc 90(5):1347
3. Kalish D, Clougherty EV (1969) J Amer Ceram Soc 52(1):26
4. Wuchina E, Opeka M, Causey S, Buesking K, Spain J, Cull A, Routbort J, Guitierrez-Mora F (2004) J Mater Sci 39:5939
5. Loehman R, Corral E, Dumm HP, Kotula P, Tandon R (2006) Sandia Report 2006–2925
6. Blum YD, Kleebe H-J (2004) J Matre Sci 39:6023
7. Anselmi-Tamburini U, Kodera Y, Gasch M, Unuvar C, Munir ZA, Ohyanagi M, Johnson S (2006) J Mater Sci 41:3097
8. Monteverde F, Melandri C, Guicciardi S (2006) Mat Chem Phys 100:513
9. Pastor H (1977) Metallic borides: preparation of solid borides – Sintering method and properties of solid bodies In: Matkovich VI (ed) Boron and refractory borides, Springer Verlag, New York
10. Bronson A, Ma Y-T, Mutso RR, Pingitore N (1992) J Electrochem Soc 139(11):3183
11. Zhu S, Fahrenholtz WG, Hilmas GE, Zhang SC (2007) Mat Sci Eng A 459:167
12. Zhang SC, Hilmas GE, Fahrenholtz WG (2006) J Am Ceram Soc 89(5):1544
13. Talmy IG, Zaykoski JA, Opeka MM, Smith AH (2006) J Mat Res 21(10):2593
14. Silvestroni L, Sciti D (2007) Scri Mater 57:165
15. Monteverde F, Bellosi A (2003) J Electrochem Soc 150(11):B552
16. Kang ES, Jang CW, Lee CH, Kim CH (1989) J Amer Ceram Soc 72(10):1868
17. Zdaniewski WA, Brungard NL (1992) J Amer Ceram Soc 75(10):2849
18. Drouin D, Couture AR, Gauvin R, Hovington P, Horny P, Demers H (2001) MonteCarlo Simulation of electron trajectory in solids (CASINO) vers. 2.41
19. McHale AE (1994) Phase diagrams for Ceramists Vol X, Fig. 8799, The American Ceramic Soc. (ed), p 126
20. Baik S, Becher P (1987) J Amer Ceram Soc 70(8):527
21. Roine A, HSC 6.0 for Windows, Outokumpu Research Oy, Pori (Finland)